

Activation Parameters for the Reactive Intermediates Relevant to Carbonylation Catalysts Based on Cobalt Carbonyls¹

Steve M. Massick, Torsten Büttner, and Peter C. Ford*

Department of Chemistry and Biochemistry, University of California, Santa Barbara, Santa Barbara, California 93106

Received September 18, 2002

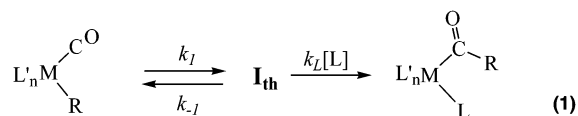
Time-resolved spectroscopic techniques have been used to prepare and to interrogate transient species that are models for reactive intermediates in cobalt-catalyzed hydroformylation. Flash photolysis of acetylcobalt carbonyl complexes of the type $\text{RC(O)Co(CO)}_3(\text{PR}'_3)$ (**A**; $\text{R} = \text{CH}_3, \text{CD}_3, \text{or } \text{C}_2\text{H}_5$; $\text{R}' = \text{Ph or } ^t\text{Bu}$) leads to CO photodissociation to give the “unsaturated” intermediate $[\text{RC(O)Co(CO)}_2(\text{PR}'_3)]$ (**I**), which decays by two competitive pathways, alkyl migration to the cobalt to give $\text{RCO(CO)}_3\text{PR}'_3$ (**M**) and reaction with CO to re-form **A**. With the perdeuterioacetyl complex ($\text{R} = \text{CD}_3, \text{R}' = \text{Ph}$), rate constants both of CO trapping (k_{CO}) and of methyl migration (k_{M}) were just slightly smaller than those of the perprotio analogue ($k^h/k^d = 1.04 \pm 0.01$ and 1.07 ± 0.09 , respectively). Thus, any stabilization of the “vacant” coordination site of **I** by agostic interactions with the acetyl methyl group appears to be kinetically insignificant, consistent with the previous conclusion (*Inorg. Chem.* **2000**, *39*, 3098–3106) that this site is stabilized by an η^2 -coordinated carbonyl. Changing the phosphine ligand has a greater influence on the kinetics of **I**. The species generated by the flash photolysis of the trialkyl phosphine complex $\text{CH}_3\text{C(O)Co(CO)}_3(\text{P}(^t\text{Bu})_3)$ exhibited a much larger k_{M} than was the case for the PPh_3 analogue, although there was little difference in the k_{CO} values. Similarly, k_{M} proved to be sensitive to the nature of **R** as demonstrated by the slower alkyl migration (at 298 K) for the intermediate formed by CO photodissociation from the propionyl complex $\text{C}_2\text{H}_5\text{C(O)Co(CO)}_3\text{PPh}_3$ relative to the acetyl analogue. Nonetheless, all these intermediates displayed analogous time-resolved infrared spectra and general kinetics behavior in benzene solution (implying common mechanisms for decay), so it is concluded that all are present as the η^2 -chelated acyl structure under these conditions.

Introduction

Carbon monoxide “migratory insertion” into metal–alkyl bonds is the key C–C bond formation pathway in catalytic carbonylations such as acetic acid synthesis from methanol, alkene hydroformylation, etc.² Since the discovery of cobalt carbonyl hydroformylation catalysts in 1938, homogeneous carbonylation has grown to major economic importance, and

CO can be considered the most important C₁ building block of the chemical industry.

Alkylmetal carbonyl complexes have been extensively probed as models for this fundamental class of organometallic reactions.^{3–5} Such studies suggest a mechanism in which reversible alkyl migration to a *cis*-carbonyl leads to a reactive intermediate **I**_{th}, which subsequently reacts with a ligand **L** in solution (eq 1).

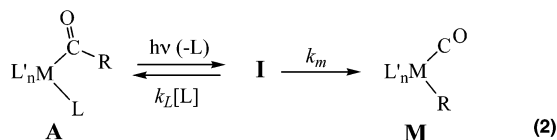


Intermediates such as **I**_{th} are rarely observable directly owing to their low steady-state concentrations. The strategy used in this laboratory for characterizing the structure and reactivity of such transient species starts with an acyl complex, i.e., the product of the thermal reaction. Photodis-

* Author to whom correspondence should be addressed. E-mail: ford@chem.ucsb.edu.

- (1) (a) Taken in part from the Diplomarbeit, by T.B., submitted in June 2000 to the Chemisch Geowissenschaftliche Fakultät, Institut für Anorganische und Analytische Chemie, Friedrich-Schiller-Universität Jena, Germany. (b) Reported in part at the 217th ACS National Meeting, Anaheim, CA, March 1999; INORG 168.
- (2) (a) Parshall, G. W.; Ittel, S. D. *Homogeneous Catalysis*; John Wiley & Sons: New York, 1992. (b) Cornils, B.; Herrmann, W. A. *Applied homogeneous catalysis with organometallic compounds: a comprehensive handbook in two volumes*; VCH: Weinheim, New York, 1996.
- (3) Collman J. P.; Hegedus, L. S.; Norton, J. R.; Finke, R. G. *Principles and Applications of Organotransition Metal Chemistry*; University Science Books: Mill Valley, CA, 1987; Chapter 6.

sociation of a ligand L from the acyl complex **A** (eq 2)



prepares a reactive intermediate **I** with the same composition as that proposed for the thermal reaction intermediate. Time-resolved spectroscopic studies are used to interrogate the nature of **I** as well as the dynamics of the reactions to give the stable acyl products and of reverse alkyl migration to give the metal alkyl complex **M**. The resulting time-resolved optical (TRO) and time-resolved infrared (TRIR) spectra under various conditions are then interpreted in terms of potential mechanisms. For example, in this manner we have probed the model systems $\text{Mn}(\text{CO})_5(\text{C}(\text{O})\text{R})$ and $\text{CpFe}(\text{CO})_2(\text{C}(\text{O})\text{R})$ ($\text{Cp} = \eta^5\text{-C}_5\text{H}_5$).^{6,7} Described here is an extension of our recent study of cobalt systems⁸ related to the phosphine-modified cobalt carbonyl catalysts used in certain industrial hydroformylation processes.²

Phosphine-modified cobalt carbonyl catalysts used for carbonylation of higher olefins have more favorable linear-to-branched selectivity but require higher temperatures than do catalysts based on the simple cobalt carbonyls.² The former also have greater tolerance of feedstock impurities and better thermal stability than do rhodium catalysts now predominant for propene hydroformylation. As a consequence, there is continuing interest in new applications of cobalt carbonyls as carbonylation catalysts.⁹ Pioneering mechanistic studies by Heck and Breslow¹⁰ of cobalt carbonyl catalyzed hydroformylation of alkenes led to the proposed catalytic cycle that has been the starting point for quantitative reaction mechanism studies with unsubstituted

and substituted cobalt carbonyl catalysts.¹¹ A key step is the migratory insertion of a CO into a Co–R bond (eq 3).



Described in the present paper are time-resolved spectroscopic investigations of the modified cobalt carbonyl complexes $\text{RC}(\text{O})\text{Co}(\text{CO})_3(\text{PR}'_3)$, where R is CH_3 , CD_3 , or Et and PR'_3 is PPh_3 or P^nBu_3 . The goal of the present study was to survey the possible effects of changing the alkyl group or the phosphine modifier on the reaction dynamics of the intermediate **I**. One concern was the possible role of agostic bonding between alkyl group C–H(D) bonds and Co in stabilizing **I**. In addition P^nBu_3 is a closer approximation (than is PPh_3) to the trialkylphosphines used in the modified cobalt carbonylation catalysts.² These studies were carried out using a high-pressure variable-temperature (HP/VT) flow cell reactor^{7c} to examine the reactivity of **I** under a wide range of CO partial pressures (P_{CO}) and temperatures in a manner that allows the accurate determination of activation parameters for the competitive decay steps.

Experimental Section

Materials. All syntheses were carried out on a vacuum line using Schlenk and cannula techniques or in an inert atmosphere box under argon. The argon used in the vacuum line was dried and deoxygenated by passage over columns of activated molecular sieves and an oxygen scavenger (Phillips catalyst on silica). Dicobalt octacarbonyl was purchased from Strem Chemicals, and the phosphines PPh_3 and P^nBu_3 and acid chlorides $\text{CD}_3\text{C}(\text{O})\text{Cl}$ and $\text{C}_2\text{H}_5\text{C}(\text{O})\text{Cl}$ were purchased from Aldrich. All solvents were from Fischer Chemicals and dried by refluxing with sodium and distilling under a N_2 atmosphere.¹² Research grade carbon monoxide gas (99.995% purity from Spectra Gases) was used without further purification.

Syntheses. The phosphine-modified acylcobalt carbonyl complexes $\text{RC}(\text{O})\text{Co}(\text{CO})_3(\text{PR}'_3)$ (**A**) used in the flash photolysis studies were prepared from $\text{Co}_2(\text{CO})_8$ in overall yields near 50% according to published methods.¹³ The products were characterized by NMR and FTIR spectroscopy.

Solutions for TRIR Experiments. The calculated amounts of cobalt complex were transferred into a Schlenk-type flask in the drybox, where they were stored. Following evacuation for a few minutes to remove residual solvents or gases, the desired solvent was added using a cannula. Prior to that, the solvent was dried and distilled under argon and afterward degassed either by the freeze–pump–thaw (f–p–t) technique or simply by repeated evacuation. The solution concentration was generally about 3 mM. With a path length of 0.5 mm, this gave an optical absorbance at the 355 nm

- (4) (a) Mawby, R. J.; Basolo, F.; Pearson, R. G. *J. Am. Chem. Soc.* **1964**, *86*, 3994–3999. (b) Calderazzo, F. *Angew. Chem., Int. Ed. Engl.* **1977**, *16*, 299–311. (c) Cawse, J. N.; Fiato, R. A.; Pruett, R. L. *J. Organomet. Chem.* **1979**, *172*, 405–413. (d) Flood, T. C. *Top. Stereochem.* **1981**, *12*, 37–118. (e) Webb, S.; Giandomenico, C.; Halpern, J. *J. Am. Chem. Soc.* **1986**, *108*, 345–347. (f) Cavell, K. J. *Coord. Chem. Rev.* **1996**, *155*, 209–243.
- (5) Jordon, R. B. *Reaction Mechanisms of Inorganic and Organometallic Systems*, 2nd ed.; Oxford University Press: New York, 1998.
- (6) (a) Belt, S. T.; Ryba, D. W.; Ford, P. C. *J. Am. Chem. Soc.* **1991**, *113*, 9524–9528. (b) Boese, W. T.; Lee, B. L.; Ryba, D. W.; Belt, S. T.; Ford, P. C. *Organometallics* **1993**, *12*, 4739–4741. (c) Boese, W. T.; Ford, P. C. *Organometallics* **1994**, *13*, 3525–3531. (d) Boese, W. T.; Ford, P. C. *J. Am. Chem. Soc.* **1995**, *117*, 8381–8391.
- (7) (a) McFarlane, K. L.; Ford, P. C. *Organometallics* **1998**, *17*, 1166–1168. (b) McFarlane, K. L.; Lee, B.; Fu, W. F.; van Eldik, R.; Ford, P. C. *Organometallics* **1998**, *17*, 1826–1834. (c) Massick, S. M.; Ford, P. C. *Organometallics* **1999**, *18*, 4362–4366.
- (8) Massick, S.; Rabor, J.; Elbers, S.; Marhenke, J.; Bernhard, S.; Schoonover, J.; Ford, P. C. *Inorg. Chem.* **2000**, *39*, 3098–3106.
- (9) (a) Rathke, J. W.; Klinger, R. J.; Krause, T. R. *Organometallics* **1991**, *10*, 1350–1355. (b) Knifton, J. F.; Lin, J. J. *J. Mol. Catal.* **1993**, *81*, 27–36. (c) Piotti, M. E.; Alper, H. *J. Am. Chem. Soc.* **1996**, *118*, 111–116. (d) Kramarz, K. W.; Klingler, R. J.; Fremgen, D. E.; Rathke, J. W. *Catal. Today* **1999**, *49*, 339–352. (e) Miguel, S.; Zeigler, T. *Organometallics* **1996**, *15*, 2611 and references therein. (f) Rossi, L.; Piacenti, F.; Bianchi, M.; Frediani, P.; Salvini, A. *Eur. J. Inorg. Chem.* **1999**, 67–68. (g) Goh, S. K.; Marynick, D. S. *Organometallics* **2002**, *22*, 2262–2267. (h) Allmendinger, M.; Eberhardt, R.; Luinstra, G.; Reiger, B. *J. Am. Chem. Soc.* **2002**, *124*, 5646–5647.
- (10) Heck, R. F.; Breslow, D. S. *J. Am. Chem. Soc.* **1962**, *84*, 2499–2502.

- (11) (a) Martin, J. T.; Baird, M. C. *Organometallics* **1983**, *2*, 1073–1078. (b) Kovacs, I.; Ungvary, M.; Marko, L. *Organometallics* **1986**, *5*, 209–215. (c) Roe, D. C. *Organometallics* **1987**, *6*, 942–946. (d) Pino, P.; Major, A.; Spindler, F.; Tannenbaum, R.; Bor, G.; Horvath, I. T. *J. Organomet. Chem.* **1991**, *417*, 65–76. (e) Borovikov, M. S.; Kovacs, I.; Ungvary, F.; Sisak, A.; Marko, L. *Organometallics* **1992**, *11*, 1576–1579. (f) Bartik, T.; Krummling, T.; Happ, B.; Sieker, A.; Marko, L.; Boese, R.; Ugo, R.; Zucchi, C.; Palyi, G. *Catal. Lett.* **1993**, *19*, 383–389. (g) Klingler, R. J.; Rathke, J. W. *J. Am. Chem. Soc.* **1994**, *116*, 4772–4785. (h) Rathke, J. W.; Klinger, R. J., II; R. E. G.; Kramarz, K. W.; Woelk, K. *Prog. NMR Spectrosc.* **1997**, *30*, 209–253.
- (12) Riddick, J. A.; Bunger, W. B.; Sakano, T. K. *Organic Solvents Physical Properties and Methods of Purification*, 4th ed.; John Wiley & Sons: New York, 1986; Vol. II.
- (13) Lindner, E.; Zipper, M. *Chem. Ber.* **1974**, *107*, 1444–1455. (b) Roe, D. C. *Organometallics* **1987**, *6*, 942–946.

laser excitation wavelength of ~ 0.75 and initial IR absorbances of 0.3–0.4 for the most intense of the terminal carbonyl stretching bands of the parent complex. The sample was transferred into the Parr autoclave of the HP/VT flow system^{7c} using a gastight syringe under a CO atmosphere. The gas mixture at a specific pressure was introduced, and the solution was stirred for at least 1 h to guarantee complete equilibration. Concentrations of CO were calculated from published solubility data.¹⁴ TRIR experiments were carried out using flowing solutions to minimize complications arising from product accumulation. The temperature throughout the flow system and sample cell was regulated.

TRIR Instrumentation. Time-resolved infrared studies were conducted on an experimental apparatus described previously.^{6d,8,15} The probe system is based upon diode IR lasers mounted in a Spectra Physics/Laser Analytics model SP5731 laser head and a CVI Digikrom model 240 monochromator and provides a tunable IR probe laser source in the frequency range 1500–2200 cm^{-1} . The probe beam was focused to a 7 mm diameter spot and overlapped at the plane of the sample cell with the 355 nm pump pulse from a Lumonics HY600 Nd:YAG laser. The transmitted intensity of the IR probe beam was focused to fill the 1 mm^2 active area of a Fermionics model PV-8-1 photovoltaic Hg/Cd/Te detector. A Fermionics model PVA 500-50 preamplifier enhanced the detector signal prior to digitization by a LeCroy 9400 oscilloscope. The average intensity of the pretrigger region (-2 to 0 μs) was taken as I_0 to calculate absorbance according to $\text{Abs}(t) = -\log(I(t)/I_0)$.

Results and Discussion

Treatment and Quality of TRIR Kinetics Data. Data were accumulated for flowing solutions by recording the temporal signal intensity of the IR photodiode immediately before and after laser pulse excitation of the solution. Usually data from 40 to 60 shots were acquired and encapsulated to a single data set that was transformed to absorbance vs time curves with good signal-to-noise ratios. Under CO, these curves fit well to simple exponential decays from which first-order rate constants k_i were calculated. Generally, the mean of 26 k_i values so determined was used to provide the “observed rate constant” k_{obsd} values reported here for a particular compound at a specific P_{CO} and T (see Figure S-1 in the Supporting Information). An experiment was considered relevant only if the internal deviation among the 26 k_i values was small and random rather than systematic. This level of data analysis ensured that no trend caused by insufficient stirring, which could result in inhomogeneous CO concentrations, was present. Figure 1 represents one of the 26 acquisitions used to calculate the k_{obsd} for the decay of the transient seen at 1915 cm^{-1} upon 355 nm flash photolysis of $\text{CD}_3\text{C}(\text{O})\text{Co}(\text{CO})_3(\text{PPh}_3)$ (A_{CD_3}) in benzene under 100 psig of CO ($P_{\text{CO}} = 7.85$ bar) and at 45 °C. For this particular experiment the decay constant was determined to be $(9.73 \pm 0.03) \times 10^5 \text{ s}^{-1}$, while the mean value for

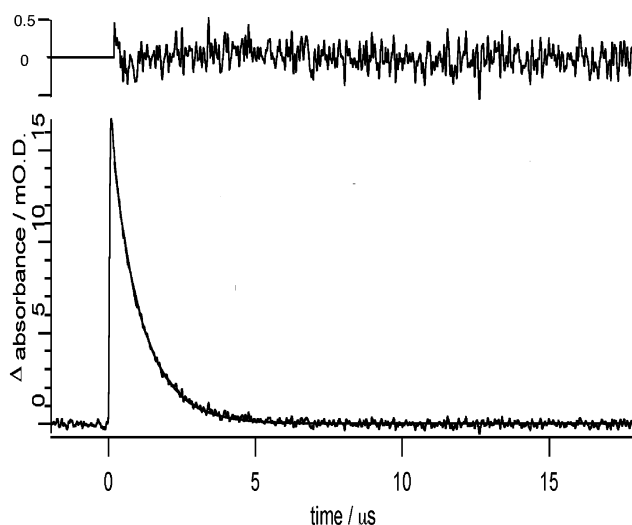
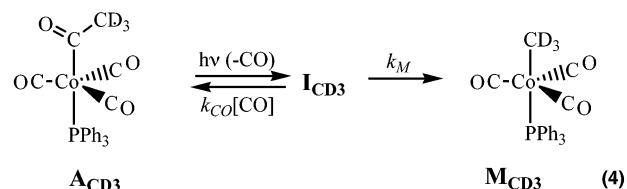


Figure 1. Temporal IR absorbance change at 1915 cm^{-1} (milli absorbance units, mOD) after signal-averaged 40-shot acquisition for the 355 nm flash photolysis of A_{CD_3} in benzene solution under 100 psig of CO and at 45 °C. For this particular experiment k_{obsd} was calculated to be $(9.73 \pm 0.03) \times 10^5 \text{ s}^{-1}$ from the exponential fit, which is also shown. The quality of the fit is illustrated by the residual plotted at the top of the figure at a scale of ± 0.5 mOD.

k_{obsd} was determined to be $(9.63 \pm 0.11) \times 10^5 \text{ s}^{-1}$. The relative standard deviations of the k_{obsd} values were generally lower than 2%.

Flash Photolysis Studies of $\text{CD}_3\text{C}(\text{O})\text{Co}(\text{CO})_3(\text{PPh}_3)$ (A_{CD_3}). An earlier report⁸ from this laboratory using both variable single frequency and step scan FTIR techniques demonstrated that 355 nm excitation of $\text{CH}_3\text{C}(\text{O})\text{Co}(\text{CO})_3(\text{PPh}_3)$ (A_{CH_3}) leads to CO photodissociation to give a reactive intermediate I_{CH_3} . Analysis of the TRIR spectra concluded that there were but two detectable products from the decay of I_{CH_3} ,⁸ A_{CH_3} re-formed by CO trapping of I_{CH_3} and the alkyl complex M_{CH_3} from the competitive methyl migration from the acyl group to the metal. The analogous scheme (eq 4) was assumed for the perdeuterio analogue.



According to this model, the rate constant for the decay of I_{CD_3} would be expected to follow the behavior $k_{\text{obsd}} = k_{\text{M}} + k_{\text{CO}}[\text{CO}]$. Variation of $[\text{CO}]$ was accomplished by applying CO pressures up to 160 psig (11.96 bar absolute) in the HP/VT flow system. P_{CO} was determined by taking the vapor pressure of benzene into account, and the mole fractions χ and concentrations (mol/L) in solution were calculated. The reaction dynamics were probed for 7–10 different $[\text{CO}]$ values at each temperature studied. Plots of k_{obsd} vs $[\text{CO}]$ obtained for a specific temperature were linear with slopes k_{CO} and intercepts k_{M} as shown in the inset of Figure 2 and in Figure S-2 of the Supporting Information. Table 1 lists k_{M} and k_{CO} values determined at six temperatures over the range 20–45 °C and compares these to the rate constants

(14) Concentrations of CO in various solvents were corrected for differences in solubility: *IUPAC Solubility Data Series: Carbon Monoxide*; Cargill, R. W., Ed.; Pergamon Press: New York, 1990; Vol. 43.

(15) (a) Ford, P. C.; Bridgewater, J. S.; Lee, B. *Photochem. Photobiol.* **1997**, *65*, 57–64. (b) DiBenedetto, J. A.; Ryba, D. W.; Ford, P. C. *Inorg. Chem.* **1989**, *28*, 3503–3507. (c) Bridgewater, J. S.; Schoonover, J. R.; Netzel, T. L.; Massick, S. M.; Ford, P. C. *Inorg. Chem.* **2001**, *40*, 1466–1476.

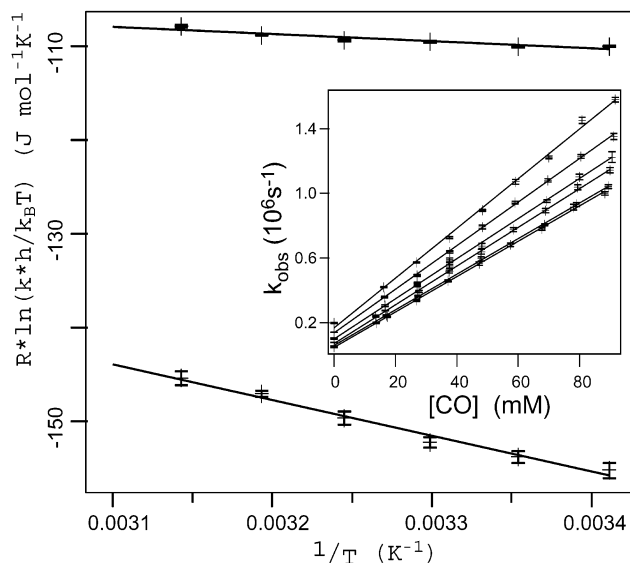
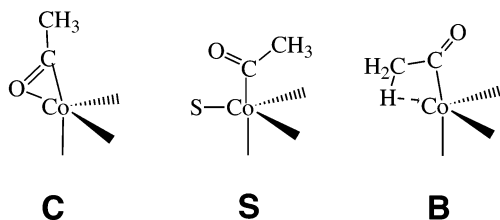


Figure 2. Eyring plots for k_M (lower) and for k_{CO} (upper) determined for the decay of the transient I_{CD_3} generated by flash photolysis of A_{CD_3} in benzene. Inset: k_{obsd} vs $[CO]$ for individual temperatures ranging from 20 (lowest) to 45 °C.

measured for decay of the perprotio analogue I_{CH_3} in benzene. Eyring plots (Figure 2) for the k_{CO} and k_M values give the activation parameters ΔH^\ddagger and ΔS^\ddagger for the two decay pathways (Table 1).

The data in Table 1 indicate that there is little isotope effect on either the k_M or k_{CO} pathways of **I**. A very small “normal” kinetic isotope effect (i.e., $k^h/k^d > 1.00$) was observed at 298 K for both k_M and k_{CO} ($k_M^h/k_M^d = 1.07 \pm 0.09$ and $k_{CO}^h/k_{CO}^d = 1.04 \pm 0.01$). This was also reflected in the activation parameters ΔH^\ddagger and ΔS^\ddagger , which are (within experimental uncertainty) the same for the two decay pathways for the intermediates I_{CH_3} and I_{CD_3} (Table 2).

Three possible structures for I_{CH_3} are illustrated below as **C**, **S**, and **B**. The absence of significant changes in k_{CO} as the solvent was varied argued against the I_{CH_3} being the



solvento complex **S**, especially in a relatively weakly coordinating solvent such as benzene.⁸ Shifts in the acetyl group ν_{CO} frequency indicated that this is still intact in I_{CH_3} , probably as the η^2 -coordinated structure as illustrated by **C**. A recent density functional calculation^{9f} confirms that **C** is likely to be the lowest energy structure of an intermediate having the related composition $CH_3C(O)Co(CO)_3$, barring strongly donating solvents. The very small normal kinetic isotope effect for both pathways adds further credence to the assignment of I_{CH_3} and I_{CD_3} as having the η^2 -acetyl-chelated structure **C**. An alternative would be a bidentate configuration stabilized by an agostic interaction between

the methyl C–H(D) bonds and the metal center (**B**). If the latter were the case, then an “inverse” isotope effect (i.e., $k^h/k^d < 1.00$) would be expected owing to the changes in the C–H(D) vibrational zero-point energies in going from the agostic coordinated **B** to transition states of the pathways leading either to the η^1 -coordinated $-CH_3$ of **M** (k_M) or to the η^1 -bonded acetyl of **A** (k_{CO}).¹⁶ The small normal k^h/k^d values are consistent with modest weakening of methyl group normal modes as the CH_3 moves through the reaction transition states. Such a result might imply a more negative charge on the CH_3 group at the k_M transition state in the course of moving from **C** to **M**. Alternatively, this might reflect agostic bonding during the course of the migratory insertion mechanism; however, we are disinclined to place much emphasis on such a small effect.

Flash Photolysis of $CH_3C(O)Co(CO)_3P(\eta Bu)_3$ (A_{PBu_3}) and $C_2H_5C(O)Co(CO)_3PPh_3$ (A_{Et}). The intermediate I_{PBu_3} was generated by 355 nm flash photolysis of A_{PBu_3} in 308 K benzene ($P_{CO} \approx 4$ atm), and the carbonyl region transient TRIR spectrum was recorded using a 400 ns window for data collection. Bleaching of bands characteristic of A_{PBu_3} was noted, as well as the appearance of ν_{CO} bands for I_{PBu_3} at $1903(\pm 2)$ and $1640(\pm 2)$ cm^{-1} , both of which disappeared with lifetimes of ~ 1 ms under these conditions. On this time frame, a long-lived absorbance at ~ 1935 cm^{-1} characteristic of the methyl analogue M_{PBu_3} was also apparent. The bands for I_{PBu_3} were analogous to those reported previously for the PPh_3 analogue I_{CH_3} ⁸ but were shifted to somewhat lower frequencies (~ 10 cm^{-1}) owing to the greater electron-donating ability of the trialkylphosphine.

Kinetics data were acquired by following the exponential disappearance of the 1903 cm^{-1} band of I_{PBu_3} to obtain k_{obsd} values at seven CO concentrations over the range 0 to ~ 90 mM for each of four temperatures (298, 308, 313, and 318 K). Values of k_M and k_{CO} were extracted from the intercepts and slopes, respectively, of linear k_{obsd} vs $[CO]$ plots. Eyring plots of these data (Figure S-3 in the Supporting Information) gave the ΔH^\ddagger and ΔS^\ddagger values. The k_M and k_{CO} values at 298 K and the respective activation parameters for the reactions leading to decay of I_{PBu_3} are summarized in Table 2. While k_M is significantly larger than seen for I_{CH_3} , consistent with a smaller value of ΔH_M^\ddagger , the rates and activation parameters for the k_{CO} step are little affected.

The carbonyl region TRIR spectrum of the intermediate I_{Et} generated by 355 nm flash photolysis of propionyl complex A_{Et} in benzene was recorded using a 300 ns window for data collection. Bleaching of the ν_{CO} bands characteristic of A_{Et} and the appearance of new bands for I_{Et} at $1915(\pm 2)$ and $1632(\pm 2)$ cm^{-1} were noted. The terminal ν_{CO} band for I_{Et} matches an analogous band in the TRIR spectrum of I_{CH_3} ,

(16) (a) Calvert, R. B.; Shapley, J. R. *J. Am. Chem. Soc.* **1978**, *100*, 7726–7727. (b) Buchanan, J. M.; Stryker, J. M.; Bergman, R. G. *J. Am. Chem. Soc.* **1986**, *108*, 1537–1550. (c) Piers, W. E.; Bercaw, J. E., *J. Am. Chem. Soc.* **1990**, *112*, 9406–7. (d) Paur-Afshari, R.; Lin, J.; Schultz, R. H. *Organometallics* **2000**, *19*, 1682–1691. (e) Tanner, Martha J.; Brookhart, M.; DeSimone, J. M. *J. Am. Chem. Soc.* **1997**, *119*, 7617–7618.

Table 1. Values of k_M and k_{CO} (with Standard Deviations) for I_{CD_3} and I_{CH_3} (from Ref 8) Determined from the Linear k_{obsd} versus $[CO]$ Fits at Each Individual T Used for the Determination of the Eyring Activation Parameters ΔH^\ddagger and ΔS^\ddagger

T (°C)	k_M^d ($10^4 s^{-1}$)	k_{CO}^d ($10^7 M^{-1} s^{-1}$)	k_M^h ($10^4 s^{-1}$)	k_{CO}^h ($10^7 M^{-1} s^{-1}$)	k_M^h/k_M^d	k_{CO}^h/k_{CO}^d
20	4.5 ± 0.5	1.09 ± 0.01				
25	5.8 ± 0.5	1.10 ± 0.01	6.2 ± 0.7	1.14 ± 0.01	1.07 ± 0.09	1.04 ± 0.01
30	7.1 ± 0.5	1.20 ± 0.01	7.6 ± 0.5	1.19 ± 0.01	1.07 ± 0.07	0.99 ± 0.01
35	9.8 ± 0.8	1.24 ± 0.02	10.5 ± 0.9	1.26 ± 0.02	1.07 ± 0.09	1.02 ± 0.01
40	13.6 ± 0.6	1.35 ± 0.01	13.5 ± 0.6	1.34 ± 0.01	0.99 ± 0.05	0.99 ± 0.01
45	16.9 ± 1.2	1.45 ± 0.02	18.0 ± 0.8	1.40 ± 0.02	1.07 ± 0.06	0.97 ± 0.02
ΔH^\ddagger (kJ mol $^{-1}$)	39 ± 3	6.6 ± 1.4	40 ± 2	5.7 ± 0.4		
ΔS^\ddagger (J mol $^{-1}$ K $^{-1}$)	-23 ± 9	-88 ± 5	-19 ± 6	-91 ± 5		

Table 2. Rate Constants (298 K) and Activation Parameters for the Reactions of Flash Photolysis Generated Intermediates in Benzene Solution

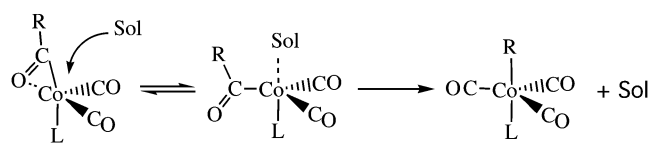
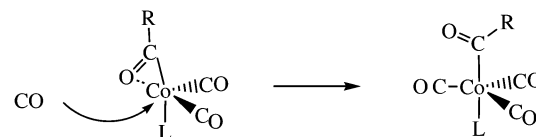
	starting complex A_{CH_3}	starting complex A_{CD_3}	starting complex A_{Et}	starting complex A_{PBu_3}
$k_{CO}(298 K)$ ($M^{-1} s^{-1}$)	$(1.14 \pm 0.01) \times 10^7$	$(1.10 \pm 0.01) \times 10^7$	$(6.1 \pm 0.1) \times 10^6$	$(8.8 \pm 0.2) \times 10^6$
ΔH_{CO}^\ddagger (kJ mol $^{-1}$)	5.7 ± 0.4	6.6 ± 1.4	6.8 ± 0.6	4.7 ± 2.8
ΔS_{CO}^\ddagger (J mol $^{-1}$ K $^{-1}$)	-91 ± 12	-88 ± 5	-92 ± 2	-96 ± 9
$k_m(298 K)$ (s^{-1})	$(6.2 \pm 0.7) \times 10^4$	$(5.8 \pm 0.5) \times 10^4$	$(2.7 \pm 0.5) \times 10^4$	$(6.3 \pm 0.1) \times 10^5$
ΔH_m^\ddagger (kJ mol $^{-1}$)	40 ± 2	39 ± 3	52 ± 5	34 ± 3
ΔS_m^\ddagger (J mol $^{-1}$ K $^{-1}$)	-19 ± 6	-23 ± 9	13 ± 15	-21 ± 9

but the acyl ν_{CO} bands for A_{Et} (1670 cm^{-1}) and I_{Et} occur at lower frequencies, respectively, than for the acetyl analogues A_{CH_3} (1679 cm^{-1}) and I_{CH_3} (1639 cm^{-1}), perhaps owing to Et being more electron donating than Me. The rate constants determined by monitoring the recovery of the A_{Et} bleach at 1670 cm^{-1} and decay of the I_{Et} absorption at 1632 cm^{-1} were in good agreement.

Kinetics data for the decay of I_{Et} were acquired by following the exponential disappearance of the 1915 cm^{-1} band to obtain k_{obsd} values at seven CO concentrations over the range 0 to $\sim 90 \text{ mM}$ for each of four temperatures (298, 308, 313, and 318 K). Values of k_M and k_{CO} were extracted for each temperature from the intercepts and slopes, respectively, of linear k_{obsd} vs $[CO]$ plots. Eyring plots of these data (Figure S-4 in the Supporting Information) gave the ΔH^\ddagger and ΔS^\ddagger values. The k_M and k_{CO} values at 298 K and the respective activation parameters for the reactions leading to decay of I_{Et} are summarized in Table 2, where it is seen that, while k_M demonstrates a larger value of ΔH_M^\ddagger for I_{Et} than for I_{CH_3} , the rates and activation parameters for the k_{CO} step are little affected.

Possible Mechanistic Implications. The TRIR data for the complexes studied are highly consistent with each other. For example, the acyl ν_{CO} band in the IR spectra of I_{CH_3} ,⁸ I_{Et} , and I_{PBu_3} is considerably less intense than the acyl ν_{CO} band of the respective starting complex **A** and is shifted about 40 cm^{-1} to lower frequency in each case. Furthermore, the consistency of the kinetics behavior summarized in Table 2 for the four species studied argues that the structures of the four respective intermediates must be analogous. As we have argued above and elsewhere,⁸ these observations indicate that **I** is present principally as the chelate **C** in each case.

The kinetics results reported in Table 2 summarize the rate constants for the bimolecular reactions of the intermediates **I** with CO to regenerate the respective **A** complexes (k_{CO}) as well as the first-order migration of the acyl R group to generate the respective alkyl complexes **M** (k_M). Our earlier studies⁸ of the reactions of I_{CH_3} demonstrated k_{CO} to

Scheme 1 Proposed Mechanisms of Methyl Migration and CO Addition Steps for **I****Alkyl migration****Carbon monoxide addition**

be relatively independent of the solvent medium, and this was partially the basis of the conclusion that I_{CH_3} is principally present as the chelate **C**. The data in Table 2 show that, for each **I** studied, k_{CO} (298 K) has a value near $10^7 M^{-1} s^{-1}$, with a very small ΔH_{CO}^\ddagger but a sizable, negative ΔS_{CO}^\ddagger . Such a pattern would be expected for a simple associative mechanism such as illustrated in Scheme 1¹⁸ for the k_{CO} pathway.

The alkyl migration rates offer somewhat greater variety, although they all fit the pattern of displaying a much larger activation enthalpy but much less negative activation entropy than does the respective CO trapping reaction. Given that in **C** the R group is poorly oriented for migration to the metal, the larger activation enthalpy may reflect the requirement of solvent involvement in the reorganization of the structure to one where migration can occur in a concerted step as illustrated in Scheme 1. Again, our earlier data⁸ demonstrated for I_{CH_3} that, unlike the relatively solvent insensitive k_{CO} values, k_M measured in benzene, dichloromethane, and THF varied by a factor of 20, the fastest rate being seen in the strongest donor THF. Although there is little difference between the ΔH_M^\ddagger and ΔS_M^\ddagger values for I_{CH_3} and I_{CD_3} , ΔH_M^\ddagger is measurably larger for I_{Et} and smaller for I_{PBu_3} . This would be consistent with the TRIR spectral data mentioned above.

One might expect the carbonyl oxygen of the propionyl group to be more basic than that of the acetyl, and hence the η^2 -carbonyl group more difficult to displace for \mathbf{I}_{Et} than for \mathbf{I}_{CH_3} . However, a peculiar aspect is that $\Delta S_{\text{M}}^\ddagger$ is surprisingly more favorable than for the other analogues, thus partially compensating for the less favorable $\Delta H_{\text{M}}^\ddagger$. In the same vein, the stronger donor character of PBU_3 relative to PPh_3 would make the cobalt center less electron accepting, which would thus bind the acetyl less strongly. This has little effect on the associative k_{CO} pathway, but does have the effect of lowering the enthalpic barrier for CH_3 migration.

Notably, the sensitivity of the k_{M} pathway to solvent is consistent with the frequent observation that the microscopic reverse, namely, the migratory insertion reaction of the type $\mathbf{M} + \text{L} \rightarrow \mathbf{A}$, which forms the acyl group from the metal alkyl, is promoted by donor solvents.^{6d,17} Similarly, rates of alkene hydroformylation catalyzed by phosphine-modified cobalt carbonyls are increased by addition of polar solvents;^{2b} however, given the complexity of the catalytic cycles, it would be difficult to attribute such an effect to any single step.

- (17) (a) Mawby, R. J.; Basolo, F.; Pearson, R. G. *J. Am. Chem. Soc.* **1964**, *86*, 3994–3999. (b) Butler, I. S.; Basolo, F.; Pearson, R. G. *Inorg. Chem.* **1967**, *6*, 2074. (c) Noack, K.; Calderazzo, F. J. *Organomet. Chem.* **1967**, *10*, 101–104. (d) Wax, M. J.; Bergman, R. G. *J. Am. Chem. Soc.* **1981**, *103*, 7028–7030. (e) Cotton, J. D.; Bent, T. L. *Organometallics* **1991**, *10*, 3156–3160.
- (18) The stereochemistry depicted in Scheme 1 is strictly conjectural for both reactions. The pathways chosen would have the minimum number of steps to give the most stable isomers in each case with the phosphine and acyl (for \mathbf{A}) or alkyl (for \mathbf{M}) groups in the *trans* axial positions.

In summary, further examination of the TRIR spectra of the reactive intermediates generated by the flash photolysis of the complexes $\text{RC(O)Co(CO)}_3(\text{PR}'_3)$ (\mathbf{A}) ($\text{R} = \text{CH}_3, \text{CD}_3$, or Et ; $\text{R}' = \text{Ph}$ or ^tBu) demonstrates that CO photodissociation leads to intermediates \mathbf{I} , for which it is concluded that the structure is the η^2 -carbonyl species \mathbf{C} in each case. These decay by two competitive pathways. The first is the simple associative addition of CO to regenerate the respective starting compound \mathbf{A} . The k_{CO} rates are essentially independent of the nature of the solvent medium (within the limits of the systems studied) and display a small activation enthalpy $\Delta H_{\text{CO}}^\ddagger$ and large and negative activation entropy $\Delta S_{\text{CO}}^\ddagger$ consistent with the proposed associative mechanism. In contrast the k_{M} rates are accelerated by donor solvents and display much larger activation enthalpies, and we conclude that this behavior reflects the intimate involvement of solvent in the transition state of the migratory pathway.

Acknowledgment. This research was sponsored by a grant (DE-FG03-85ER13317) to P.C.F. from the Division of Chemical Sciences, Office of Basic Energy Sciences, U.S. Department of Energy. T.B. acknowledges Dr. Prof. D. Walther, Friedrich-Schiller-Universität Jena, who served as Chair of the Diplomarbeit.

Supporting Information Available: A table of kinetics data for the transient decay of the reactive intermediate generated by the flash photolysis of $\text{CD}_3\text{COC(O)Co(CO)}_3(\text{PPh}_3)$ and four figures describing the results of various kinetics experiments. This material is available free of charge via the Internet at <http://pubs.acs.org>.

IC020567B